Received: 30 September 2021 | Accepted: 20 June 2022

DOI: 10.1002/vzj2.20223

Vadose Zone Journal

ORIGINAL RESEARCH ARTICLE

Development of a vadose zone advanced monitoring system: Tools to assess groundwater vulnerability

Dorothy C. Linneman | **Christopher E. Strickland** | **Delphine Appriou** | **Mark L. Rockhold** | **Jonathan N. Thomle** | **James E. Szecsody** | **Paul F. Martin** | **Vince R. Vermeul** | **Rob D. Mackley** | **Vicky L. Freedman**

Pacific Northwest National Laboratory, 902 Battelle Blvd., Richland, WA 99354, USA

Correspondence
Dorothy C. Linneman, Pacific Northwest National Laboratory, 902 Battelle Blvd., Richland, WA 99354, USA.
Email: dorothy.linneman@pnnl.gov

Assigned to Associate Editor Quirijn de Jong van Lier.

Funding information
U.S. Department of Energy Richland Operations Office under the Deep Vadose Zone – Applied Field Research Initiative. The Pacific Northwest National Laboratory is operated by Battelle Memorial Institute for the Department of Energy under Contract DE-AC05-76RL01830.

Abstract

Performing repeat pore-fluid sampling over long time-scales can provide valuable information on unsaturated zone contaminants and their potential flux to ground water. This information can be used to manage groundwater remedies and identify contaminants that need to be sequestered in the vadose zone to minimize flux to ground water. Pore-water samples are commonly used to obtain contaminant concentrations within the vadose zone, but existing methods are limited as they only provide a single sample at one location and time. The vadose zone advanced monitoring system (VZAMS) has been designed to integrate multiple technologies into a single down-borehole system that allows for sampling of pore fluids (liquid and gas) to provide information about contamination and hydraulic conditions at multiple depths (~0.3-m intervals) within a cased borehole. Testing has been completed at the laboratory scale to verify the sampling elements of VZAMS, including geochemical testing for representative contaminants known to exist at the Hanford Site, located in southeastern Washington State. Physical tests focused on the ability of the sampler to draw fluid under unsaturated conditions. Initial geochemical testing showed that the stainless steel material used with the porous cuff may affect the sampled concentrations of redox-sensitive contaminants under very dry conditions. Additional laboratory testing demonstrated that the VZAMS components are able to collect representative samples for substances of interest under expected field conditions. In this paper, the design and functionality of a novel instrument are demonstrated in support of subsequent testing in the field.

Abbreviations: DI, deionized; MIBK, methyl isobutyl ketone; PCAP, passive capillary sampler; VZAMS, vadose zone advanced monitoring system.

1 | INTRODUCTION

Movement of contamination from the unsaturated zone to the ground water creates the potential for exposure to receptors through the groundwater pathway, potentially leading to significant effects to human health and the environment. However, under natural recharge conditions, contaminant migration in the deep vadose zone at arid sites is a slow process (decades to hundreds of years) relative to groundwater transport resulting in unique challenges for characterization, monitoring, and remediation (Dresel et al., 2011; Oostrom et al., 2016).

For unsaturated soils, contaminant flux is determined by several important factors, including the recharge or deep drainage rate, and soil hydraulic properties. Water flow through the vadose zone is generally at rates determined by the unsaturated hydraulic conductivity and matric suction gradient of the sediments. Several U.S. Department of Energy legacy waste sites have contaminated deep vadose zones, including the Hanford Site (Gee et al., 2007), Idaho National Laboratory (Nimmo et al., 2004), and Los Alamos National Laboratory (Birdsell et al., 2005). Although the presence of radionuclides is a primary concern at these sites within the thick vadose zone, the fate and transport of other contaminants is also a concern, including metals (Dresel et al., 2011; Hua et al., 2007) and organic solvents (Gee et al., 2007; Oostrom & Lenhard, 2003).

Measurements related to the presence of contaminants in the unsaturated zone currently rely heavily on geochemical analyses performed on core samples obtained during drilling of groundwater monitoring wells. The use of groundwater monitoring alone does not provide information on expected arrival times of vadose zone contaminants to ground water, nor does it verify when fluxes are reduced due to a diminishing source (Dahan, 2020). Groundwater monitoring wells provide spatial and temporal contaminant concentration information that supports remediation management for the groundwater aquifer but provide no information regarding vadose zone concentrations. Groundwater contamination can be monitored at several depths in aquifer systems using multilevel samplers (Einarson & Cherry, 2002; Müller et al., 2010), but the technology has yet to be adapted in practice to unsaturated sediments.

Vadose zone cores can provide insight into geochemical and microbiological activity in contaminated sediments, which can affect the fate and transport of contaminants (Demirkanli et al., 2018; Fredrickson et al., 1993; Szecsody, Truex, et al., 2018; Truex et al., 2017). Additionally, studies of agricultural contaminant (nitrate) transport have used core samples collected at known times after fertilizer applications to examine how solutes are distributed in the vadose zone (Harter et al., 2005). While direct soil or sediment sampling can provide important characterization information, these measurements are typically limited to a single snapshot in time for any given sample location. Although repeat pore-fluid sampling is feasible in the shallow vadose zone, it is much more difficult to accomplish at sites such as Hanford where the unsaturated sediments are very thick (up to ~100 m).

Core Ideas

- A new down-borehole tool to sample vadose zone pore fluid was designed, constructed, and tested in the laboratory.
- Laboratory-scale tests demonstrate the ability of the sampler components to effectively draw fluid samples.
- The downhole tool is able to collect representative fluid samples without geochemical alteration of constituents.

Commercially available samplers are generally designed for depths <10 m, although pore-water tension samplers can be installed at greater depths (upwards of 70 m). Several authors have demonstrated successful measurements of solute flux with tension samplers in the unsaturated zone (Dahan et al., 2009; McGuire & Lowery, 1994; Sisson et al., 2011; Turkeltaub et al., 2016; Wood, 1973). These instruments use a porous plate or cup or tube geometry that is placed so that its outer surface is in contact with soil. A partial vacuum is applied to the interior that causes pore water to be drawn into the device under the condition that the vacuum does not exceed the air-entry pressure of the porous material (otherwise soil gas or air will be drawn in). Both McGuire and Lowery (1994) and Sisson et al. (2011) developed monitoring systems that used a tension sampler at a set depth coupled with moisture content and water potential measurements to evaluate solute flux. Turkeltaub et al. (2016) used multisampler methods to collect pore-water samples from multiple depths along with moisture content measurements to continuously evaluate nitrate transport through the vadose zone (Dahan et al., 2009; Rimon et al., 2007). Existing limitations with tension samplers include clogging, adsorption of analytes, and contamination by the sampler porous material (Di Bonito et al., 2008; Grossman & Udluft, 1991; McGuire et al., 1992). Sorption of solutes is generally less of a problem for Teflon and fritted glass, followed by stainless steel, with ceramic having the largest effect (Alexander et al., 2018; Jabro et al., 2008; Kim et al., 2006; McGuire et al., 1992; Rais et al., 2006; Zhu et al., 2017). Reduction of redox reactive contaminants has also been reported to occur on stainless steel (Alexander et al., 2018; Kim et al., 2006; Odaka & Ueda, 1995), although passivation of the stainless steel or use of other metal alloys

(e.g., titanium, nickel) can nearly eliminate potential redox reactions.

Passive capillary samplers (PCAPs) have also been used to measure pore-water concentrations, albeit in the shallow unsaturated zone (Frisbee et al., 2010; Holder et al., 1991; Liu et al., 2013; Peranginangin et al., 2009). The instrument operates by placing a capillary-wicking material (typically a rope made of many individual fibers) in contact with soil that introduces a hanging water column to create tension on the soil proportional to the length of the wick (Brown et al., 1986; Frisbee et al., 2010; Holder et al., 1991; Jabro et al., 2008; Knutson & Selker, 1994). Although they do not require an applied vacuum to function, PCAPs are ineffective in very dry soils with high matric potentials due to limitations on the amount of tension that can be applied. Fiberglass is commonly used for the wick material, but this material can affect the chemistry of the sample by the same adsorptive effects as discussed above for the suction samplers (Goyne et al., 2000; Perdrial et al., 2014).

Soil gases can also contribute to contaminant concentrations in ground water, making them important to measure for volatile compounds. In addition, remedies that inject gases require information on the spatial and temporal distribution of gas concentrations to determine the size, shape, and overall effectiveness of the treatment (Truex et al., 2012). Injected gases can be used for pneumatic testing and as tracers to assess field-scale, site-specific gas permeability (Truex et al., 2012). A typical gas sampling design for the vadose zone is one based on a pore-water tension sampler, consisting of a gas-permeable porous cup or tube that is attached to a tube extending to the surface (Truex et al., 2012). Nauer et al. (2013) also developed a multilevel sampling system that uses a packer system with individual sampling valves and capillaries to collect gas samples from multiple depths.

The vadose zone advanced monitoring system (VZAMS) has been developed to address the need for depth-discrete aqueous and gas phase concentration measurements for thick unsaturated sediments. The instrument is based on an existing wireline sample acquisition system used for groundwater sampling, providing ease of use for time-series sampling in the deep vadose zone by eliminating the need for tubing within the borehole. This paper describes the instrument design and laboratory testing performed to support effective deployment in the field.

2 | MATERIALS AND METHODS

To provide sampling at multiple depths along a cased wellbore, a wireline sample acquisition system (Westbay Instruments) designed for use under saturated conditions was modified for sampling in an unsaturated environment. The VZAMS instrument relies on customized well casing elements specifically engineered to sample liquid or gas, depending on operational requirements and field conditions. The liquid and gas sampling systems—also designated as "subassemblies"—are configured with an external porous membrane fixed to an internal frame that provides a docking point for the sample acquisition system. A vacuum is applied to the sample container, and the Westbay wireline tool is lowered to the desired depth and engages with the VZAMS subassembly section of the borehole casing (Figure 1). Once properly engaged with the sampler element, the port on the Westbay tool is opened to allow fluid to flow into the container. Once the fluid sample is collected into the container, the probe and container are then retrieved to the surface for further analysis.

2.1 | Design of VZAMS samplers

The VZAMS liquid and gas samplers are modified sections of well casing engineered to enable the efficient withdrawal of fluid when embedded in unsaturated sediments. Porous 316L stainless steel was used to construct the sampler cuffs as it is very resistant to corrosion under conditions such as those common in the vadose zone at legacy waste sites like Hanford. The vadose zone conditions are near-neutral in pH, low in salinity, and does not contain high concentrations of any known corrosive chemical constituents (Szecsody, Truex, et al., 2018). To maintain a high air-entry value, the liquid sampler porous metal cuff has an average pore size of 0.1 μm and is 1-mm thick. The small pores retain water and allow pore water to move through the membrane but prevent the passage of air, unless the air-entry pressure of the membrane is exceeded (at ∼70 kPa of soil-moisture tension). The gas casing subassembly has larger pore size and lower air-entry pressure to allow for gas migration. The average pore size of the gas sampler porous cuff is 40 μm. This porous cuff is manufactured twice as thick as the liquid sampler's porous cuff (2 vs. 1 mm).

The porous cuff creates a sampling contact area of approximately 64 cm^2 directly in contact with the surrounding unsaturated sediments. A series of interconnected drainage channels underlie the porous cuff (Figure 1). At the center of the drainage grid is a single small hole connecting the surface area of the porous material to the inside wall of the well casing. The total internal volume of the liquid sampler (pore volume of the porous stainless steel plus the volume of drainage channels is approximately 1.4 ml. Integral orienting and locating features (ramp and notch) are designed to align the commercial sampling tool to the sampling hole.

2.2 | Test cell and data acquisition system

A stainless steel test cell was constructed to test the performance of the VZAMS samplers at a laboratory scale. The

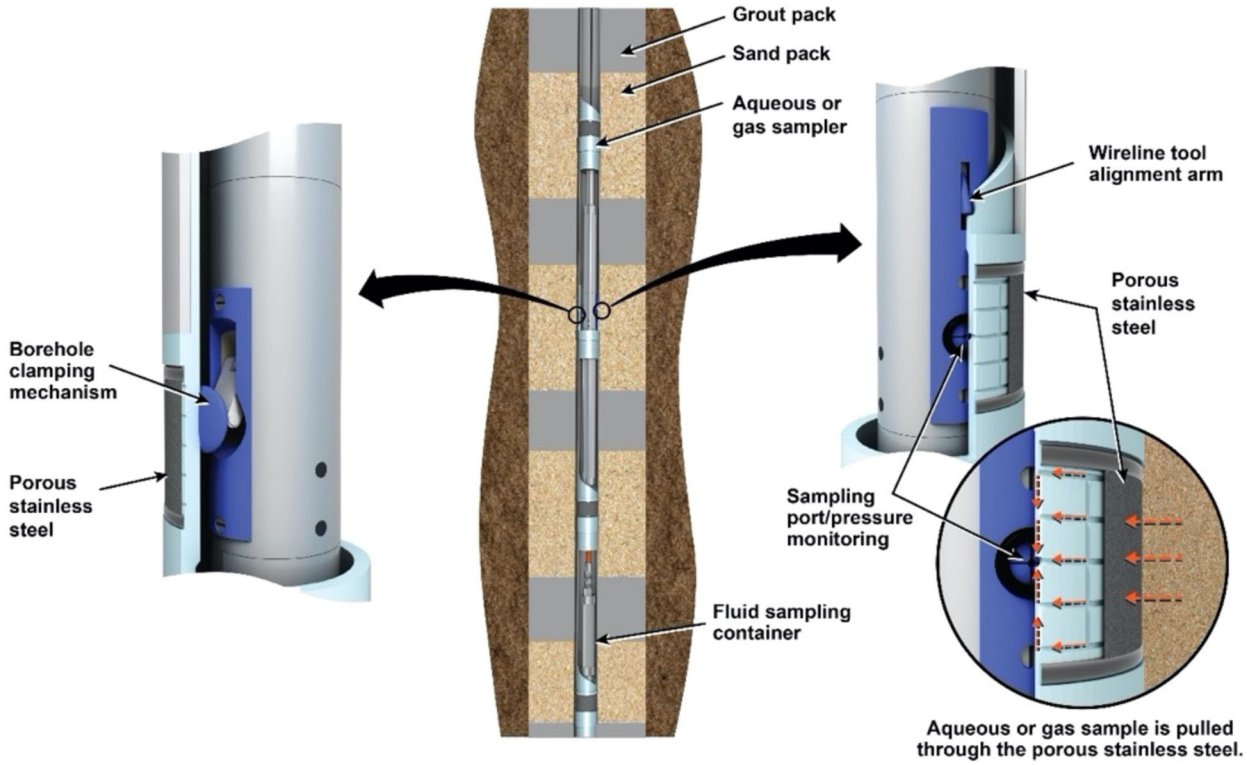

FIGURE 1 Diagram of vadose zone advanced monitoring system (VZAMS) installed in a borehole and Westbay wireline tool operation

test cell accepts the VZAMS sampler components, as shown in Figure 2, and has several ports for instrumentation and fluid circulation. The test cell assembly can be filled with 2 L of fluid or sediment and includes a stainless steel top plate that can be sealed to enclose the volume between an installed VZAMS sampler and the test cell walls.

A custom-built data acquisition system was designed for the evaluation of the physical performance of the VZAMS components prior to field deployment. The data acquisition system consists of a National Instruments CompactRIO system, which includes a programmable controller that uses Linux operating system. The MOSDAX (Westbay Instruments) commercial wireline borehole sampling probe was used to collect pore fluid from the VZAMS samplers. A Westbay Instruments MAGI II datalogger was used to log data from the wireline sampling tool.

2.3 | Laboratory performance testing

Several laboratory-based tests were carried out to evaluate the performance of the instrument prior to field installation. These experiments were particularly focused on quantifying the reactivity of the porous stainless steel with known contaminants present at the Hanford Site, for example, chromate (10–13,000 μg L^{-1}), U (10–9,500 μg L^{-1}), nitrate (0–50 mg L^{-1}), and methyl isobutyl ketone (MIBK) (0–4,000 mg L^{-1}) (Szecsody, Mitroshkov, et al., 2018). Testing included (a) measurement of the saturated hydraulic conductivity of the aqueous sampler; (b) measurement of the air-entry pressure of the aqueous sampler using multiple solutions of MIBK in water; (c) quantification of the flow rate and contact time of pore water from sediments at different water contents through the sampler; and (d) measurement of the potential contaminant interactions (i.e., sorption, reduction) with stainless steel and rubber components of the sampler.

2.3.1 | Evaluation of the hydraulic conductivity of the VZAMS porous steel

The saturated hydraulic conductivity of the porous steel of the sampler was measured to evaluate the rate at which the sampler could pull a water sample under tension, assuming the bubbling pressure of the porous steel is not exceeded. Hydraulic conductivity (K), defined by Darcy's law, measures how much fluid flows through a given cross-sectional area and length of material under a known pressure differential at steady state. Darcy's law can be expressed as:

$$\frac{Q}{A} = -K\frac{\mathrm{dh}}{\mathrm{dl}} \quad (1)$$

where Q is the flow rate, A is the surface area of the material, K is the saturated hydraulic conductivity, dh is the change in

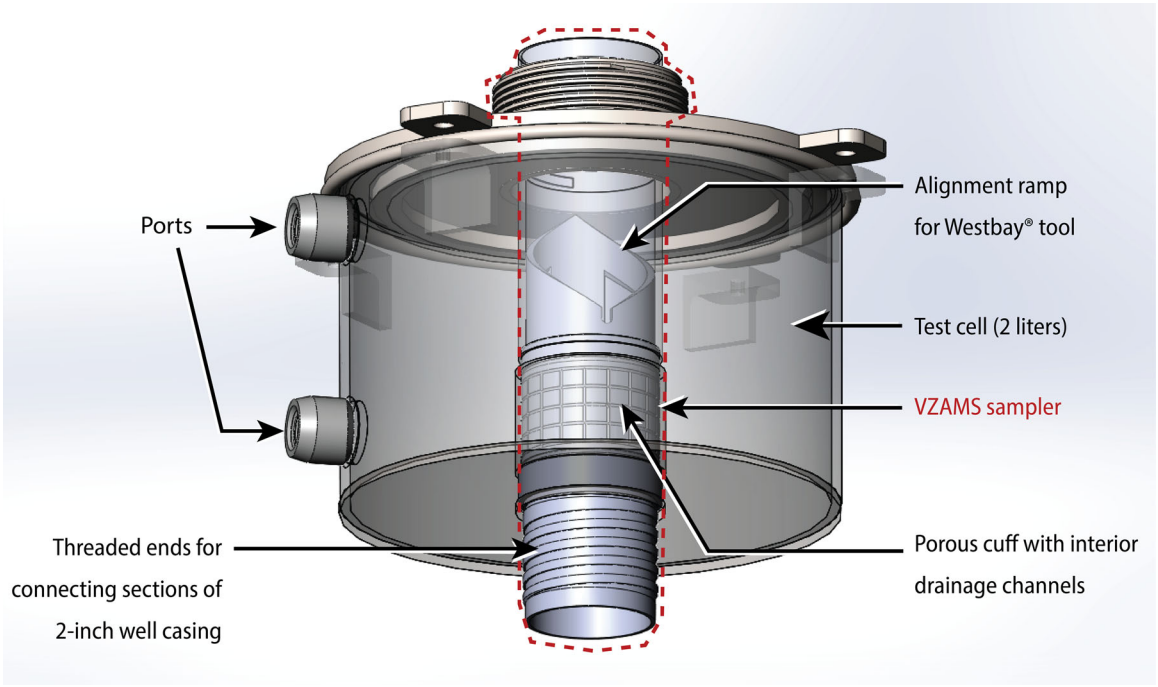

FIGURE 2 Schematic diagram of test cell assembly with vadose zone advanced monitoring system (VZAMS) sampler installed (shown as translucent to display internal structure)

hydraulic head or known pressure differential, and dl is the length of the flow path through the material. The liquid sampler subassembly was saturated overnight in deionized (DI) water. The assembly was then installed in the test cell, which was filled with DI water and left open to atmospheric pressure. The Westbay wireline tool was then engaged with the liquid subassembly. A fluid line from the outlet of the Westbay tool was connected to a collection flask located on a zeroed balance. A pressure controller was used to apply a vacuum of 100 cm of H_2O to the collection flask, and the sampling port on the Westbay tool was opened to allow fluid to flow through the porous steel cuff and through the wireline tool into the collection flask. The mass of water collected in the flask was recorded each minute for 3–5 min. This procedure was repeated for vacuums of 20–50 kPa. The rate of flow was then used with Equation 1 to calculate the saturated hydraulic conductivity of the porous steel cuff.

2.3.2 | Physical performance of the VZAMS aqueous sampler in filter pack

The nominal diameter of the VZAMS pore water and gas samplers is 5.1 cm (~2 in.) as it was designed to occupy a standard PVC well casing. The nominal diameter of a borehole is anticipated to be ~10 cm (4 in.). Filter pack material consisting of 100–200 mesh clean quartz sand is typically used to fill this annular space for well installations, alternating with layers of grout (Brown et al., 2006; Dumble et al., 2006; Einarson, 2006). Once deployed in the field, the VZAMS components would be centered in the ~1.5-m thick sand lifts between ~3-m thick cement or bentonite grout seals. Dry moisture conditions and very low surface recharge result in limited preferential annular flow along the vertical borehole. Annular flow may occur after atypical precipitation events, and sampling should not occur following heavy precipitation for risk of nonrepresentative samples. Additionally, the grout seals in the borehole annulus between the VZAMS sampler elements further minimizes preferential vertical downward flow along the borehole annulus between sampler locations. Some vertical flow can be expected within the sand lift intervals, and samples collected will be representative of average conditions along the sand interval. Placement of grout in the borehole annulus between sampler locations is also expected to improve the lateral hydraulic connection between the samplers and the adjacent sediments such that collected samples are representative of the pore fluids in the adjacent sediments.

After installation, the filter pack should be allowed to equilibrate with the conditions of the surrounding sediments prior to sample collection. The rate of this equilibration will be dictated by the moisture content and unsaturated hydraulic conductivity of the native sediments and the filter pack material. Physical and hydraulic properties of the native soils or sediments can be estimated from intact core samples collected during drilling. This characterization can be helpful in determining the filter pack material to use in the borehole annulus, and in estimating the appropriate vacuum to apply to the aqueous samplers. After equilibrating with the

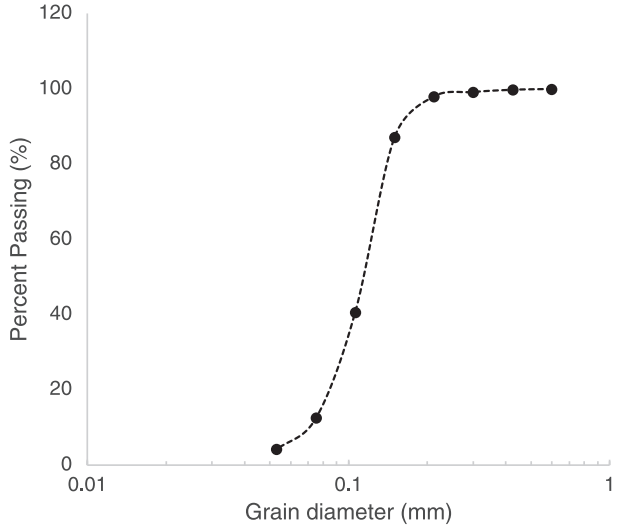

FIGURE 3 Particle-size distribution for LM 125 sand

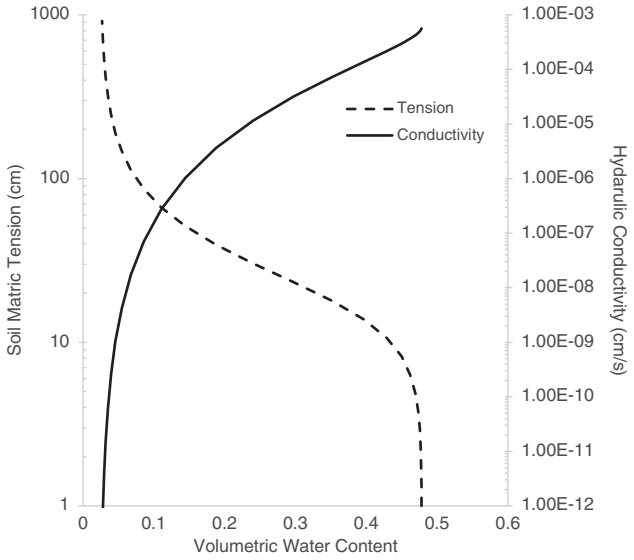

FIGURE 4 Water retention (van Genuchten, 1980) and hydraulic conductivity (Mualem, 1976) estimates for the LM 125 sand based on particle-size distribution data and hydraulic property correlation functions

surrounding sediments, water extracted by the VZAMS pore-water sampler must pass through filter pack material and be resupplied by pore water from the surrounding native sediments, such that over time, the VZAMS will effectively sample the pore water from the native sediments. Experimental data are needed to provide confidence that the VZAMS pore-water sampler will be able to effectively extract water from unsaturated filter pack materials under expected field conditions.

A target quartz sand filter pack material, LM 125, was selected for field deployment. The LM 125 sand is a locally sourced (Lane Mountain Sand Co.) clean quartz sand that is fine enough to maintain sufficient moisture to extract an aqueous sample from under expected field conditions and has high enough hydraulic conductivity to obtain a sample in a reasonable amount of time. The particle-size distribution data for this material is shown in Figure 3.

No other physical or hydraulic property data are currently available for the LM 125 sand. Therefore, hydraulic parameters for the LM 125 sand were estimated from its reported particle-size distribution and correlation functions developed from published grain size distributions and measured hydraulic properties (Carsel & Parrish, 1988). A characteristic curve of soil matric tension and hydraulic conductivity vs. volumetric water content of LM 125 sand using estimated parameters is shown in Figure 4.

Typical volumetric water contents in the subsurface at the Hanford Site are expected to range from about 0.03–0.11 with soil matric tensions ranging from about 5–50 kPa (Brown et al., 1986; Rockhold et al., 2017). Using an estimated porosity for the filter pack of 0.478, and assuming a grain density of 2.65 g cm^{-3}, the estimated dry bulk density of the LM 125 filter pack is ~1.38 g cm^{-3}. Target water contents of 4 and 8% water by weight were tested because their corresponding volumetric water contents, ~0.05 and ~0.11, respectively, are representative of field conditions.

TABLE 1 Artificial ground water used in extractions (Szecsody, Truex, et al., 2018)

Constituent	Concentration	Mass for 1 L
	mg L^{-1}	g
H_2SiO_3*nH_2O, silicic acid	15.3	0.0153
KCl, potassium chloride	8.2	0.0082
$MgCO_3$, magnesium carbonate	13	0.013
NaCl, sodium chloride	15	0.015
$CaSO_4$, calcium sulfate	67	0.067
$CaCO_3$, calcium carbonate	150	0.15

LM 125 sand was brought to moisture contents of 4 and 8% using artificial Hanford ground water (Table 1). The VZAMS aqueous sampler was saturated under a vacuum overnight in the artificial groundwater solution to ensure no air was trapped in the porous steel. The mass of the empty sample container was recorded, then the sample bottle was evacuated to a pressure of −40 kPa and the sample bottle was attached to the Westbay wireline tool. The aqueous sampler was installed in the test cell and the pre-wetted sand was then packed in the test cell to a density approximating Hanford soil bulk density. The Westbay wireline tool was then inserted into the sampler and locked into place. A tensiometer was inserted into the sand through a port in the test cell and the test cell was closed except for a small port to minimize evaporation while allowing atmospheric pressure. The valve on the Westbay wireline tool was then opened to collect a pore-water sample. Every minute,

the tensiometer pressure, the sample bottle pressure, and the pressure and temperature at the Westbay sampling port were recorded by the data acquisition system. The test was terminated when there was no longer a pressure gradient between the test cell and the sample bottle, as measured by the transducer on the sample bottle. The mass of the sample was then measured. This procedure was repeated three times for each water content for a total of six tests.

2.3.3 | Evaluation of the influence of MIBK on bubbling pressure of VZAMS aqueous sampler

The surface tension of water decreases with increasing MIBK concentration (Demond & Lindner, 1993). With concentrations of MIBK as high as 4,000 mg L^{-1} (Szecsody, Mitroshkov, et al., 2018), a reduction in bubbling pressure could potentially reduce the effective operational range of the aqueous sampler in the field. Therefore, air-entry pressure measurements of the VZAMS aqueous sampler were made in water containing varying MIBK concentrations up to 6,000 mg L^{-1}. The nominal capillary bubbling pressure of the porous stainless steel material used in the VZAMS aqueous sampler is ~70 kPa. The sampler was tested in solutions of artificial ground water, a water composition based on the geochemistry of Hanford ground water (see Table 1) with MIBK in concentrations of 1,500, 3,000, and 6,000 mg L^{-1}. The liquid sampler was sealed at both ends and inserted into a beaker of the test solution and saturated under vacuum for at least 4 h. The interior pressure of the sampler was then increased incrementally every 3 min until the air-entry pressure of the porous frit was reached and bubbles were seen on the surface of the porous material. The air-entry pressure of the porous material was recorded for each concentration of MIBK.

2.3.4 | Characterization of contaminant interaction with VZAMS sampler components

The stainless steel and rubber (O-ring) components of the VZAMS sampler were identified as components that may cause sorption or reduction of specific contaminants that are present at the Hanford waste site. For example, the 316L porous stainless steel has previously been reported to exhibit reduction of dissolved oxygen (Alexander et al., 2018; Kim et al., 2006), and so may reduce chromate and U(VI) aqueous species.

Sorption–reduction experiments were performed using selected contaminants (i.e., Cr, U, nitrate, MIBK) in artificial ground water and to evaluate potential geochemical interaction between the contaminant (or multiple contaminants) and the stainless steel or rubber VZAMS components. Different types of batch experiments were performed, which included: (a) measurement of U and Cr interactions over time (0–530 h); (b) measurement of individual contaminant U, Cr, NO_3, and MIBK removal from solution (from sorption and reduction) at different contaminant concentration; (c) measurement of coupled contaminant removal from solution to evaluate competition for adsorption–reduction sites; and (d) measurement of U or Cr adsorption–reduction in the presence of high MIBK concentration.

The individual and coupled contaminant batch experiments were conducted over 24 h at a solute concentration of 1.0 g ml^{-1} with Cr at 20–2,000 μg L^{-1}, U at 10–1,000 μg L^{-1}, NO_3 at 10–100 mg L^{-1}, and MIBK at 10–3,000 mg L^{-1} in artificial ground water (Table 1). Kinetic batch experiments were conducted at a stainless steel/water ratio concentration of 0.68 g ml^{-1} with 360 μg L^{-1} chromate and 230 μg L^{-1} U and sampling times at 0.03, 3, 21, 66, 166, 334, 500, and 530 h. At the end of the kinetic experiment, the porous stainless steel was separated from the remaining fluid into two vials and solid phase Cr and U was extracted with (a) an ion exchange solution to extract adsorbed contaminants [1.0 mol L^{-1} $Mg(NO_3)_2$], and (b) 2% nitric acid to dissolve and oxidize reduced or precipitated Cr and U surface phases (i.e., $Cr^{III}(OH)_3$ and $U^{IV}O_2$). Some experiments were conducted with duplicates.

The contaminant concentrations in the initial (i.e., unreacted) solution and after reaction(s) with solids were measured by different analytical methods. The MIBK concentration was measured by gas chromatography-mass spectrometry by head sampling. Aqueous U was measured by two methods: (a) inductively coupled plasma-optical emission spectrometry (ICP-OES) for total aqueous U, and (b) kinetic phosphorescence analysis for U(VI) aqueous species (Brina & Miller, 1992). The purpose of the dual analysis was to confirm adsorbed species (if any) are U(VI) aqueous species and acid-extracted samples from the surface are U(VI) or U(IV) species. Aqueous Cr was also measured by two methods: (a) ICP-OES for total aqueous Cr, and (b) colorimetric analysis by reaction with 1,5- diphenylcarbazide for aqueous Cr(VI) species, following Hach method 8023 (based on Environmental Protection Agency Method 7196A) (Pflaum & Howick, 1956). The aqueous nitrate concentration was measured by ion chromatography.

For contaminants that exhibited only sorption and no reduction, a Langmuir adsorption isotherm,

$$S = MKC/(1 + KC) \quad (2)$$

was used to fit the experimental data, where S is the solute surface phase concentration (in mg kg^{-1}), C is the solute final aqueous concentration (in μg ml^{-1}), M is the total number of sites (mg kg^{-1}), and K is the concentration-specific adsorption affinity parameter. A distribution coefficient (K_d) was also calculated at each concentration using the relationship

$$K_d = S/C = MK/(1 + KC) \quad (3)$$

The Mott Metallurgical porous 316L stainless steel used to construct the porous cuffs had a measured dry bulk density (ρ_b) of 6.53 g ml^{-1} and porosity (θ) of 0.184. Rubber density was estimated at 1.2 g cm^{-3} and a porosity of 0.24. These values were used to calculate the retardation factor using:

$$R_f = 1 + \rho_b K_d/\theta \quad (4)$$

Additional batch experiments were performed on alternate materials to evaluate whether another available porous material may be more suitable for use in environments containing redox-sensitive contaminants. These experiments followed the same procedure as the stainless steel experiments, and were performed on porous Ni, Ti, and ceramic.

Further testing was performed on the stainless steel prototype sampler to evaluate the ability of the liquid sampler element to collect chemically representative samples based on the flow rates measured during the filter pack experiments. Artificial groundwater solution (Table 1) containing a known quantity of chromate was pumped through the liquid sampler element at fixed flow rates, which encompass the range of expected sampling rates under field conditions (2 ml d^{-1} to 2 ml h^{-1}). At a flow rate of 2 ml h^{-1}, samples were collected every 3 h for a total of six samples. At a flow rate of 2 ml d^{-1}, samples were collected after 48, 96, and 144 h. Measures were taken to reduce evaporation of the samples during collection to ensure accurate chemical analysis. The samples collected were then analyzed for Cr content and compared against the starting (control) concentration to determine whether Cr was removed from the solution through interaction with the porous stainless steel. The ICP-OES analysis was used to measure total aqueous chromium on the collected samples as well as several control samples.

2.3.5 | Physical performance testing of the gas sampler

The VZAMS gas sampling subassembly was installed in the test cell. The Westbay wireline tool was then seated in the sampling port on the gas sampler subassembly, and the sample bottle was evacuated to a pressure of −40 kPa. The test cell was then purged with N_2 gas for 20 min before the port on the Westbay tool was opened to draw a sample of N gas from the test cell. Commercial Dräger oxygen sampling tubes and pump were used to assess the presence of oxygen in the gas sample bottle. The presence of oxygen would indicate gas drawn into the sample bottle from a source other than the test cell. Figure 5 shows a schematic illustration of the method used for testing the gas samples. The test was repeated five times for a total of six analyses. Three samples of ambient air were also tested for oxygen levels.

3 | RESULTS

3.1 | Hydraulic conductivity

The flow rate of water through the porous steel cuff at pressure differentials of 10–50 kPa is shown in Table 2. The mean flow rate (cm^3 min^{-1}) over each 5-min test duration was calculated and is also shown in Table 2.

The surface area and thickness of the porous steel cuff are 63.88 cm^2 and 0.1 cm, respectively. These values are used with Equation 1 to calculate the mean hydraulic conductivity of the sampler material (see Table 3). The mean saturated hydraulic conductivity of the porous cuff is 1.49×10^{-6} cm s^{-1}.

3.2 | Filter pack performance tests

As noted previously, the experimentally determined saturated hydraulic conductivity of the porous stainless steel in the VZAMS pore-water sampler is approximately 1.5×10^{-6} cm s^{-1}. The sampling rates for the six tests (three tests at each water content) in filter pack ranged from about 2 ml d^{-1} up to nearly 2 ml h^{-1}. Results demonstrated that collection times could be several days, especially at lower water contents, as demonstrated by the 4% water content by weight sample requiring several days to collect approximately 3 ml of water. Additionally, some variability in sample mass collected was observed for the tests at 8% water content by weight, which may indicate the potential for the area adjacent to the porous cuff to desaturate faster than fluid moving to replace the extracted pore fluid, thereby limiting the conductivity of the filter pack near the sampling location. In addition to moisture content, additional factors such as soil composition may affect the sampling time required. Therefore, the appropriate sample duration is site-specific and should be determined based on the soil characteristics at the site of interest. For typical Hanford soil conditions, a container pressure of −40 kPa and sampling duration of 72 h is appropriate for collecting liquid samples.

3.3 | Influence of MIBK on bubbling pressure

The air-entry pressure of the liquid sampling subassembly at concentrations of MIBK of 0, 1,500, 3,000, and 6,000 mg L^{-1} in artificial groundwater solution (Table 1) was measured.

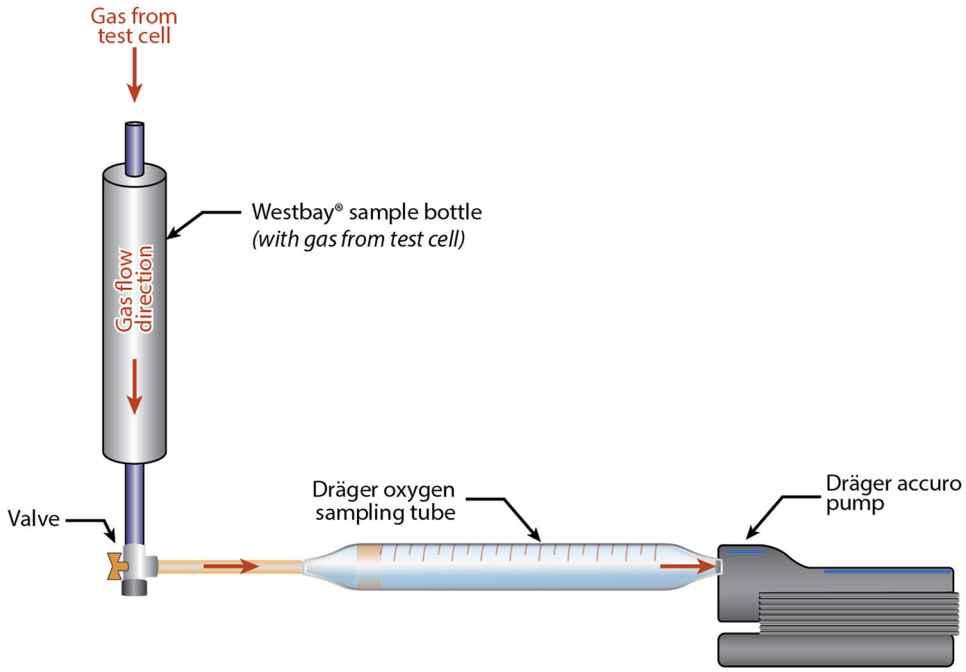

FIGURE 5 Schematic diagram of a setup for using Dräger gas sampling system to measure concentrations of O_2 in gas samples collected from the vadose zone advanced monitoring system (VZAMS) gas sampler subassembly

TABLE 2 Flow rate of deionized water through the porous stainless cuff over time at different pressure differentials

	Volume of deionized water collected per minute				
Interval	**10 kPa**	**20 kPa**	**30 kPa**	**40 kPa**	**50 kPa**
min	ml				
1	7.56	14.03	17.8	18.96	23.94
2	7.32	14.04	17.66	18.41	22.76
3	7.23	13.66	16.09	18.01	21.7
4	7.19	13.48	16.03	17.39	20.41
Mean	7.325	13.8025	16.895	18.1925	22.2025

TABLE 3 Measured sampling rates and calculated hydraulic conductivity values for different pressure differentials

Pressure differential	**Sampling rate**	***K***
kPa	$cm^3\ min^{-1}$	$cm\ s^{-1}$
10	7.325	1.89×10^{-6}
20	13.8025	1.78×10^{-6}
30	16.895	1.46×10^{-6}
40	18.1925	1.18×10^{-6}
50	22.2025	1.15×10^{-6}
	Mean	1.49×10^{-6}

The air-entry pressure of the porous sampling material was not reduced at 1,500 mg L^{-1} MIBK. At 3,000 mg L^{-1}, the air-entry pressure was reduced to 67.5 kPa, and at 6,000 mg L^{-1} the air-entry pressure was nominally reduced to 60 kPa. The highest measured concentration of MIBK in Hanford sediments is 4,000 mg L^{-1}, and even at higher concentrations the air-entry pressure is still higher than the greatest estimated matric tension in the Hanford vadose zone (Szecsody, Mitroshkov, et al., 2018). Based on these results, it is not anticipated that concentrations of MIBK will affect the ability of the VZAMS to effectively pull a water sample in the field.

3.4 | Contaminant interaction with stainless steel and rubber components

3.4.1 | MIBK interactions

A minimal amount of MIBK sorption was measured to the porous stainless steel with calculated K_d values of 0.02 ml g^{-1} (at 10 mg L^{-1} MIBK) to 0.06 L kg^{-1} (at 1,000 mg L^{-1} MIBK).

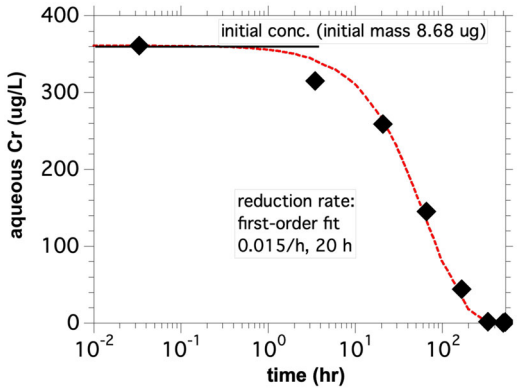

FIGURE 6 Reduction of 360 mg L^{-1} chromate with porous stainless steel

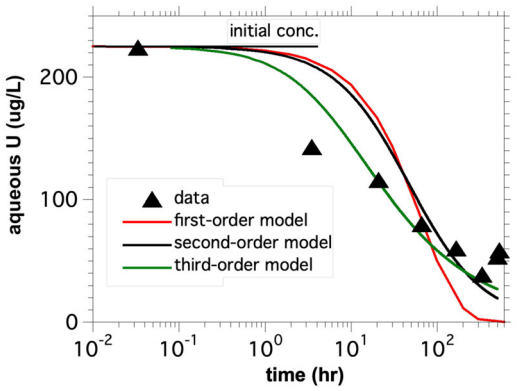

FIGURE 7 Uranium reduction rate on porous stainless steel

3.4.2 | Nitrate interactions

No nitrate sorption or reduction was measured with interactions with the porous stainless steel component of the VZAMS sampler. For experiments at low (10 mg L^{-1}) nitrate concentration, the final nitrate concentration after 24 h of contact with the stainless steel was 22–30% higher than the initial nitrate concentration, indicating some nitrate leaching from the stainless steel surface. This nitrate is presumed to be left over from a cleaning/passivating step during the manufacturing process (ASTM International, 2017).

3.4.3 | Chromium interactions

A batch time-course experiment was conducted to quantify the rate of chromate aqueous species removal from solution and determine if the surface species were adsorbed or reduced. Chromate initially at a concentration of 360 µg L^{-1} (with U, as described in the following section) was removed within 330 h of contact with the porous material, and the rate was fitted with a first-order reduction reaction with a 20-h half-life and reduction rate of 1.53×10^{-4} mmol h^{-1} kg^{-1} (Figure 6). This chromate removal was consistent with reduction rather than sorption, and proof of reduction vs. sorption was verified with recovery of adsorbed chromate and precipitated Cr(III).

Additional chromate interaction experiments with stainless steel and rubber components were conducted in batch systems at different chromate (and other solute) concentrations. Over a period of 24 h, chromate removal decreased with increasing concentration (from 20 to 2,000 µg L^{-1}), indicating a rate limitation for the porous stainless steel reduction of chromate. Chromate removal from solution by rubber components was small (K_d = 1.2 L kg^{-1}) and attributed to sorption. The presence of MIBK did not alter the chromate removal rate.

3.4.4 | Uranium interactions

A batch time-course experiment was also conducted to quantify the rate of U aqueous species (initially at 224 µg L^{-1}) removal from solution in the presence of chromate (see previous section). The U was removed from solution at a slower rate than chromate, which left some U(VI) remaining in aqueous solution at 530 h. The rate of removal could not be fit with a first- or second-order model (red and black lines, respectively, Figure 7), but could be fit with a third-order model (green line). The U(VI) reduction to U(IV)O_2 precipitates is a second-order electron transfer reaction, so in total a third-order reaction. Although the 12-h half-life was more rapid than chromate, the calculated reduction rate was smaller (8.0×10^{-5} mmol h^{-1} kg^{-1}) because of the lower starting mass (0.022 µmol U vs. 0.167 µmol Cr).

Extraction of adsorbed U surface phases on the porous stainless steel using the Mg-nitrate ion exchange solution showed that 0.25% of U was U(VI), and thus was likely present on the surface as adsorbed Ca-uranyl-carbonate species. The total U recovered from the surface with the 2% nitric acid extraction was 120% of initial U(VI) mass, so nearly all uranium removed from solution was reduced and precipitated on the stainless steel surface.

Additional U interaction experiments with stainless steel and rubber components were conducted in batch systems at different U (and other solute) concentrations. Over a period of 24 h, U removal decreased with increasing concentration (from 10 to 1,000 µg L^{-1}), indicating a rate limitation for the porous stainless steel reduction of U, similar to that observed for chromate. Uranium removal from solution by rubber components was very small (K_d = 0.36 L kg^{-1}) and attributed to sorption. The presence of MIBK did not alter the U removal rate.

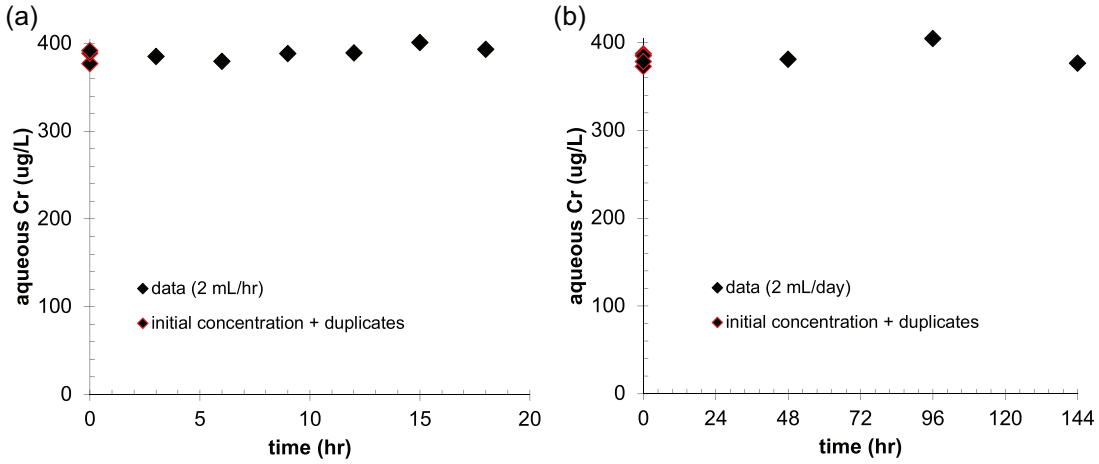

FIGURE 8 Chromate concentration over time of samples collected through vadose zone advanced monitoring system (VZAMS) porous stainless steel at fixed flow rates of (a) 2 ml h^{-1} and (b) 2 ml d^{-1}

3.4.5 | Contaminant interactions with alternate porous materials

Results of additional batch testing show that reduction of U and chromate occurs with all tested porous materials (i.e., Ti, Ni, ceramic), at varying rates. Rates of reduction of U and chromate by Ni and Ti were similar or even slightly faster than 316 stainless steel. Sorption of U and chromate to porous ceramic was also observed. These results are presented in the Supplemental Materials.

3.4.6 | Chromate interactions with stainless steel at expected flow rates

Based on the results of the performance testing of the fluid sampler in filter pack materials, it was determined that the sampling rate could vary from as low as 2 ml d^{-1} under very dry conditions to as high as 2 ml h^{-1} at higher water content conditions. Further testing to evaluate the interaction of contaminants with the liquid sampler element at expected sample flow rates show no measurable loss of Cr at expected sampling rates. Initial geochemical testing showed that chromate had the fastest removal rate of the contaminants of interest. Therefore, this additional chromate testing demonstrates that at expected flow rates, no measurable loss of any redox-sensitive contaminants of interest is expected. The measured values of chromate concentration after 3, 6, 9, 12, 15, and 18 h at flow rate of 2 ml h^{-1} as well as after 48, 96, and 144 h at flow rate 2 ml d^{-1} were all within the measurement uncertainty of the control measurements (Figure 8).

Based on the volume of the liquid sampler porous cuff (1.4 ml), the expected range of field sampling rates correspond to a fluid contact time with the porous material of 0.7 h to approximately 17 h. Given the observed reduction rate of U and chromate and the results of the additional chromate testing, at higher water content in the vadose zone, the sample contact time with the porous stainless steel will result in minimal influence of chromate or U reduction. At very low water contents, however, the extended contact time between the pore fluid and the porous stainless steel during collection of liquid samples could result in some observed loss of U or Cr through reduction by the porous stainless steel. However, any indication of contaminant presence would still provide information on subsurface contaminant conditions. Contaminant flux through the vadose zone would also be very small under such dry conditions.

3.5 | Physical performance testing of the VZAMS gas sampler

Tests of the gas sampling subassembly were performed to ensure that the system would pull a gas sample from the region of interest and not be susceptible to air leaks. The tests were designed such that the test cell was initially filled with N gas. The extracted gas was analyzed for oxygen, based on the assumption that little to no oxygen would be detected if the sampler was actually pulling (N) gas from the target region. Otherwise, significant concentrations of oxygen would be measured, which would indicate air leaks. The commercial Dräger sampling tubes used to detect the presence of oxygen gas in the sample bottle have a measurement range of 5–23% O_2 and are accurate to within ±5%. Three control measurements of O_2 gas by volume performed on the ambient air range from 16 to 17% O_2, while all six samples collected from the test cell measured less than the minimum threshold of 5% O_2, indicating that the VZAMS instrument successfully draws a gas sample from the targeted source free of significant leaks.

4 | CONCLUSIONS

This paper describes the first phase of laboratory testing for a multilevel pore-fluid sampling system. Results of the physical performances tests indicated that the VZAMS components are working as expected, with the sampler able to extract water from unsaturated sediments at relatively dry conditions. Testing of the instrument once installed in the field will provide additional confidence in the laboratory test results. Based on the laboratory tests, the length of time to draw a sample of sufficient volume under very dry conditions can take several days. For example, at 4% water content by weight, approximately 3 ml of liquid sample was collected from the filter pack in 114 h. Such a limited sample volume may be sufficient for some contaminants if diluted, but could be prone to erroneous chemical analysis results, depending on the analytes of interest and method of analysis. Larger quantities of water were extracted in less time at a higher water content, as expected. Minimum sampling time is dependent on the hydrologic conditions in the subsurface. When deployed in the field, these approximate sampling times as determined from laboratory testing can be used to determine the appropriate duration of sample collection from each sampling location.

Redox-insensitive contaminants (i.e., Sr-90, Cs-137, tritium, MIBK) or nonprecipitating reduction contaminants (i.e., iodate to iodide) are not affected by the stainless steel used in the prototype instrument. However, initial laboratory testing identified a need to perform further experiments to constrain the chemical interactions between the porous sampler material and redox-sensitive contaminants (i.e., Cr, U). Different porous materials including Ni, Ti, and ceramic were tested to evaluate their chemical performance in Hanford conditions and exhibited similar results with reduction of chromate and U when exposed to the different porous materials over long periods of time. Additionally, measurements of chromate loss in sampled fluid using the prototype stainless steel instrument showed no measurable loss of contaminants when sampling at flow rates representative of expected field conditions. Measurable reduction of redox-sensitive contaminants could result under extremely dry conditions where the contact time between fluid and porous material is very long. However, it has been demonstrated that the VZAMS instrument collects representative fluid samples from unsaturated soils with volumetric moisture content as low as 0.03, indicating that the system is ready for installation and testing in the field. Long-term collection of pore-fluid samples at multiple locations/depths within the deep vadose zone made possible with this system can provide important information about contaminant flux to the water table, and guide remediation actions.

ACKNOWLEDGMENTS

Funding for this work was provided by the U.S. Department of Energy Richland Operations Office under the Deep Vadose Zone – Applied Field Research Initiative. The Pacific Northwest National Laboratory is operated by Battelle Memorial Institute for the Department of Energy under Contract DE-AC05-76RL01830.

AUTHOR CONTRIBUTIONS

Dorothy C. Linneman: Data curation; Formal analysis; Investigation; Methodology; Validation; Visualization; Writing – original draft; Writing – review & editing. Christopher E. Strickland: Conceptualization; Funding acquisition; Investigation; Resources; Supervision; Writing – review & editing. Delphine Appriou: Project administration; Resources; Supervision; Visualization; Writing – original draft; Writing – review & editing. Mark L. Rockhold: Rockhold: Data curation; Formal analysis; Investigation; Methodology; Resources; Supervision; Validation; Writing – review & editing. Jonathan N. Thomle: Methodology; Project administration; Resources; Supervision; Writing – review & editing. James E. Szecsody: Data curation; Formal analysis; Investigation; Methodology; Validation; Writing – original draft; Writing – review & editing. Paul F. Martin: Investigation; Methodology; Resources; Validation; Visualization; Writing – review & editing. Vince R. Vermeul: Conceptualization; Funding acquisition; Investigation; Methodology; Resources; Supervision. Rob D. Mackley: Funding acquisition; Project administration; Resources; Supervision; Writing – review & editing. Vicky L. Freedman: Conceptualization; Funding acquisition; Project administration; Resources; Supervision; Writing – review & editing.

CONFLICT OF INTEREST

The authors declare no conflict of interest.

ORCID

Dorothy C. Linneman https://orcid.org/0000-0002-7535-2428

Jonathan N. Thomle https://orcid.org/0000-0002-1221-2292

REFERENCES

ASTM International. (2017). *Standard practice for cleaning, descaling, and passivation of stainless steel parts, equipment, and systems* (A380/A380M-17). ASTM International.

Alexander, C., Liu, C., Alshanoon, A., Katona, R., Kelly, R., Carpenter, J., Bryan, C., & Schindelholz, E. (2018). Oxygen reduction on stainless steel in concentrated chloride media. *Journal of the Electrochemical Society*, *165*, C869–C877. https://doi.org/10.1149/2.0181813jes

Birdsell, K. H., Newman, B. D., Broxton, D. E., & Robinson, B. A. (2005). Conceptual models of vadose zone flow and transport beneath the Pajarito Plateau, Los Alamos, New Mexico. *Vadose Zone Journal*, *4*(3), 620–636. https://doi.org/10.2136/vzj2004.0172

Brina, R., & Miller, A. G. (1992). Direct detection of trace levels of uranium by laser-induced kinetic phosphorimetry. *Analytical Chemistry*, *64*(13), 1413–1418. https://doi.org/10.1021/ac00037a020

Brown, C. F., Serne, R. J., Bjornstad, B. N., Horton, D. G., Lanigan, D. C., Clayton, R. E., Valenta, M. M., Vickerman, T. S., Kutnyakov, I. V., Geiszler, K. N., Baum, S. R., Parker, K. E., & Lindberg, M. J. (2006). *Characterization of vadose zone sediments below the C tank farm: Borehole C4297 and RCRA Borehole 299-E27-22* (PNNL-15503, Rev. 1). U.S. Department of Energy.

Brown, K. W., Thomas, J. C., & Holder, M. W. (1986). *Development of a capillary wick unsaturated zone pore water sampler (Cooperative Agreement CR812316-01-0)*. U.S. Environmental Protection Agency.

Carsel, R. F., & Parrish, R. S. (1988). Developing joint probability distributions of soil water retention characteristics. *Water Resources Research*, *24*(5), 755–769. https://doi.org/10.1029/WR024i005p00755

Dahan, O. (2020). Vadose zone monitoring as a key to groundwater protection [conceptual analysis]. *Frontiers in Water*, *2*(61), 599569. https://doi.org/10.3389/frwa.2020.599569

Dahan, O., Talby, R., Yechieli, Y., Adar, E., Lazarovitch, N., & Enzel, Y. (2009). In situ monitoring of water percolation and solute transport using a vadose zone monitoring system. *Vadose Zone Journal*, *8*(4), 916–925. https://doi.org/10.2136/vzj2008.0134

Demirkanli, D. I., Truex, M. J., Szecsody, J. E., Snyder, M. M., Moran, J. J., Nims, M. K., Lawter, A. R., Resch, C. T., Saunders, D. L., Qafoku, N. P., Baum, S. R., & Williams, B. D. (2018). *Contaminant attenuation and transport characterization of 200-DV-1 operable unit sediment samples from boreholes C9497, C9498, C9603, C9488, and C9513* (PNNL-27524). U.S. Department of Energy.

Demond, A. H., & Lindner, A. S. (1993). Estimation of interfacial tension between organic liquids and water. *Environmental Science & Technology*, *27*(12), 2318–2331. https://doi.org/10.1021/es00048a004

Di Bonito, M., Breward, N., Crout, N., Smith, B., & Young, S. (2008). Overview of selected soil pore water extraction methods for the determination of potentially toxic elements in contaminated soils: Operational and technical aspects. In B. De Vivo, H. E. Belkin, & A. Lima (Eds.), *Environmental geochemistry* (pp. 213–249). Elsevier.

Dresel, P. E., Wellman, D. M., Cantrell, K. J., & Truex, M. J. (2011). Review: Technical and policy challenges in deep vadose zone remediation of metals and radionuclides. *Environmental Science & Technology*, *45*(10), 4207–4216. https://doi.org/10.1021/es101211t

Dumble, P., Fuller, M., Beck, P., & Sojka, P. (2006). Assessing contaminant migration pathways and vertical gradients in a low-permeability aquifer using multilevel borehole systems. *Land Contamination & Reclamation*, *14*, 699–712. https://doi.org/10.2462/09670513.698

Einarson, M. D. (2006). Multi-level ground water monitoring. In D. M. Nielsen (Ed.), *Practical handbook of ground water monitoring* (pp. 807–848). CRC Press.

Einarson, M. D., & Cherry, J. A. (2002). A new multilevel ground water monitoring system using multichannel tubing. *Groundwater Monitoring & Remediation*, *22*(4), 52–65. https://doi.org/10.1111/j.1745-6592.2002.tb00771.x

Fredrickson, J. K., Brockman, F. J., Bjornstad, B. N., Long, P. E., Li, S. W., McKinley, J. P., Wright, J. V., Conca, J. L., Kieft, T. L., & Balkwill, D. L. (1993). Microbiological characteristics of pristine and contaminated deep vadose sediments from an arid region. *Geomicrobiology Journal*, *11*(2), 95–107. https://doi.org/10.1080/01490459309377938

Frisbee, M. D., Phillips, F. M., Campbell, A. R., Hendrickx, J. M. H., & Engle, E. M. (2010). Modified passive capillary samplers for collecting samples of snowmelt infiltration for stable isotope analysis in remote, seasonally inaccessible watersheds 2: Field evaluation. *Hydrological Processes*, *24*(7), 834–849. https://doi.org/10.1002/hyp.7524

Gee, G. W., Oostrom, M., Freshley, M. D., Rockhold, M. L., & Zachara, J. M. (2007). Hanford site vadose zone studies: An overview. *Vadose Zone Journal*, *6*, 899–905. https://doi.org/10.2136/vzj2006.0179

Goyne, K. W., Day, R. L., & Chorover, J. (2000). Artifacts caused by collection of soil solution with passive capillary samplers. *Soil Science Society of America Journal*, *64*(4), 1330–1336. https://doi.org/10.2136/sssaj2000.6441330x

Grossman, J., & Udluft, P. (1991). The extraction of soil water by the suction-cup method: A review. *Journal of Soil Science*, *42*(1), 83–93. https://doi.org/10.1111/j.1365-2389.1991.tb00093.x

Harter, T., Onsoy, Y. S., Heeren, K., Denton, M., Weissmann, G., Hopmans, J. W., & Horwath, W. R. (2005). Deep vadose zone hydrology demonstrates fate of nitrate in eastern San Joaquin Valley. *California Agriculture*, *59*(2), 124–132. https://doi.org/10.3733/ca.v059n02p124

Holder, M., Brown, K. W., Thomas, J. C., Zabcik, D., & Murray, H. E. (1991). Capillary-wick unsaturated zone soil pore water sampler. *Soil Science Society of America Journal*, *55*(5), 1195–1202. https://doi.org/10.2136/sssaj1991.03615995005500050001x

Hua, B., Deng, B., Thornton, E. C., Yang, J., & Amonette, J. E. (2007). Incorporation of chromate into calcium carbonate structure during coprecipitation. *Water, Air, and Soil Pollution*, *179*(1), 381–390. https://doi.org/10.1007/s11270-006-9242-7

Jabro, J. D., Kim, Y., Evans, R. G., Iversen, W. M., & Stevens, W. B. (2008). Passive capillary sampler for measuring soil water drainage and flux in the vadose zone: Design, performance, and enhancement. *Applied Engineering in Agriculture*, *24*(4), 439–446. https://doi.org/10.13031/2013.25145

Kim, Y. P., Fregonese, M., Mazille, H., Feron, D., & Santarini, G. (2006). Study of oxygen reduction on stainless steel surfaces and its contribution to acoustic emission recorded during corrosion processes. *Corrosion Science*, *48*(12), 3945–3959. https://doi.org/10.1016/j.corsci.2006.03.006

Knutson, J. H., & Selker, J. S. (1994). Unsaturated hydraulic conductivities of fiberglass wicks and designing capillary wick pore-water samplers. *Soil Science Society of America Journal*, *58*(3), 721–729. https://doi.org/10.2136/sssaj1994.03615995005800030012x

Liu, Z., Flury, M., Zhang, Z. F., Harsh, J. B., Gee, G. W., Strickland, C. E., & Clayton, R. E. (2013). Transport of Europium colloids in vadose zone lysimeters at the semiarid Hanford site. *Environmental Science & Technology*, *47*(5), 2153–2160. https://doi.org/10.1021/es304383d

McGuire, P. E., & Lowery, B. (1994). Monitoring drainage solution concentrations and solute flux in unsaturated soil with a porous cup sampler and soil moisture sensors. *Groundwater*, *32*(3), 356–362. https://doi.org/10.1111/j.1745-6584.1994.tb00651.x

McGuire, P. E., Lowery, B., & Helmke, P. A. (1992). Potential sampling error: Trace metal adsorption on vacuum porous cup samplers. *Soil Science Society of America Journal*, *56*(1), 74–82. https://doi.org/10.2136/sssaj1992.03615995005600010012x

Mualem, Y. (1976). A new model for predicting the hydraulic conductivity of unsaturated porous media. *Water Resources Research*, *12*(3), 513–522. https://doi.org/10.1029/WR012i003p00513

Müller, K., Vanderborght, J., Englert, A., Kemna, A., Huisman, J. A., Rings, J., & Vereecken, H. (2010). Imaging and characterization of solute transport during two tracer tests in a shallow aquifer using electrical resistivity tomography and multilevel groundwater samplers. *Water Resources Research*, *46*(3). https://doi.org/10.1029/2008WR007595

Nauer, P. A., Chiri, E., & Schroth, M. H. (2013). Poly-use multi-level sampling system for soil-gas transport analysis in the vadose zone. *Environmental Science & Technology*, *47*(19), 11122–11130. https://doi.org/10.1021/es401958u

Nimmo, J. R., Rousseau, J. P., Perkins, K. S., Stollenwerk, K. G., Glynn, P. D., Bartholomay, R. C., & Knobel, L. L. (2004). Hydraulic and geochemical framework of the Idaho national engineering and environmental laboratory vadose zone. *Vadose Zone Journal*, *3*(1), 6–34. https://doi.org/10.2113/3.1.6

Odaka, K., & Ueda, S. (1995). Outgassing reduction of type 304 stainless steel by surface oxidation in air. *Journal of Vacuum Science & Technology A*, *13*(3), 520–523. https://doi.org/10.1116/1.579777

Oostrom, M., & Lenhard, R. J. (2003). Carbon tetrachloride flow behavior in unsaturated Hanford caliche material: An investigation of residual nonaqueous phase liquids. *Vadose Zone Journal*, *2*(1), 25–33. https://doi.org/10.2136/vzj2003.2500

Oostrom, M., Truex, M. J., Last, G. V., Strickland, C. E., & Tartakovsky, G. D. (2016). Evaluation of deep vadose zone contaminant flux into groundwater: Approach and case study. *Journal of Contaminant Hydrology*, *189*, 27–43. https://doi.org/10.1016/j.jconhyd.2016.03.002

Peranginangin, N. P., Richards, B. K., & Steenhuis, T. S. (2009). Assessment of vadose zone sampling methods for detection of preferential herbicide transport. *Hydrology and Earth System Science Discussion*, *2009*, 7247–7285. https://doi.org/10.5194/hessd-6-7247-2009

Perdrial, J. N., Perdrial, N., Vazquez-Ortega, A., Porter, C., Leedy, J., & Chorover, J. (2014). Experimental assessment of passive capillary wick sampler suitability for inorganic soil solution constituents. *Soil Science Society of America Journal*, *78*(2), 486–495. https://doi.org/10.2136/sssaj2013.07.0279

Pflaum, R. T., & Howick, L. C. (1956). Spectrophotometric determination of potassium with sodium tetraphenylborate. *Analytical Chemistry*, *28*(10), 1542–1544. https://doi.org/10.1021/ac60118a012

Rais, D., Nowack, B., Schulin, R., & Luster, J. (2006). Sorption of trace metals by standard and micro suction cups in the absence and presence of dissolved organic carbon. *Journal of Environmental Quality*, *35*(1), 50–60. https://doi.org/10.2134/jeq2005.0040

Rimon, Y., Dahan, O., Nativ, R., & Geyer, S. (2007). Water percolation through the deep vadose zone and groundwater recharge: Preliminary results based on a new vadose zone monitoring system. *Water Resources Research*, *43*(5), W05402. https://doi.org/10.1029/2006WR004855

Rockhold, M. L., Zhang, Z. F., & Bott, Y. (2017). Alternative conceptual models of the subsurface at WMA-C *(PNNL-24740)*. Pacific Northwest National Laboratory.

Sisson, J. B., Schafer, A. L., & Hubbell, J. M. (2011). Vadose zone monitoring system for site characterization and transport modeling. *MRS Online Proceedings Library*, *608*(1), 161. https://doi.org/10.1557/PROC-608-161

Szecsody, J., Truex, M., Lee, B., Strickland, C. E., Moran, J., Snyder, M., Resch, C. T., Lawter, A., Zhong, L., Gartman, B., Saunders, D., Baum, S., Leavy, I. I., Horner, J., Williams, B. D., Christiansen, B. B., McElroy, E. M., Nims, M. K., Clayton, R., & Appriou, D. (2018). *Geochemical, microbial, and physical characterization of 200-DV-1 operable Unit B-complex cores from boreholes C9552, C9487, and C9488 on the Hanford site central plateau*. U.S. Department of Energy, Office of Scientific and Technical Information.

Szecsody, J. E., Mitroshkov, A. V., Demirkanli, D. I., Truex, M. J., Plymale, A. E., Resch, C. T., Thompson, C. J., & Zhong, L. (2018). *Geochemical and microbial processes for methyl isobutyl ketone (MIBK) in Hanford 200 area subsurface sediments* (PNNL-28012). U.S. Department of Energy.

Truex, M. J., Oostrom, M., Strickland, C. E., Johnson, T. C., Freedman, V. L., Johnson, C. D., Greenwood, W. J., Ward, A. L., Clayton, R. E., Lindberg, M. J., Peterson, J. E., Hubbard, S., Chronister, G. B., & Benecke, M. W. (2012). *Deep vadose zone treatability test for the Hanford central plateau: Soil desiccation pilot test results* (PNNL-21369). U.S. Department of Energy.

Truex, M. J., Szecsody, J. E., Qafoku, N., Strickland, C. E., Moran, J. J., Lee, B. D., Snyder, M. M. V., Lawter, A. R., Resch, C. T., Gartman, B. N., Zhong, L., Nims, M. K., Saunders, D. L., Williams, B. D., Horner, J. A., Leavy, I. I., Baum, S. R., Christiansen, B. B., Clayton, R. E., … Striluk, M. L. (2017). *Contaminant attenuation and transport characterization of 200-DV-1 operable unit sediment samples* (PNNL-26208). U.S. Department of Energy.

Turkeltaub, T., Kurtzman, D., & Dahan, O. (2016). Real-time monitoring of nitrate transport in the deep vadose zone under a crop field – Implications for groundwater protection. *Hydrology and Earth System Sciences*, *20*(8), 3099–3108. https://doi.org/10.5194/hess-20-3099-2016

van Genuchten, M. T. (1980). A closed-form equation for predicting the hydraulic conductivity of unsaturated soils. *Soil Science Society of America Journal*, *44*(5), 892–898. https://doi.org/10.2136/sssaj1980.03615995004400050002x

Wood, W. W. (1973). A technique using porous cups for water sampling at any depth in the unsaturated zone. *Water Resources Research*, *9*(2), 486–488. https://doi.org/10.1029/WR009i002p00486

Zhu, M., Zhu, L., Wang, J., Yue, T., Li, R., & Li, Z. (2017). Adsorption of Cd(II) and Pb(II) by in situ oxidized Fe(3)O(4) membrane grafted on 316L porous stainless steel filter tube and its potential application for drinking water treatment. *Journal of Environmental Management*, *196*, 127–136. https://doi.org/10.1016/j.jenvman.2017.02.073

SUPPORTING INFORMATION

Additional supporting information can be found online in the Supporting Information section at the end of this article.

How to cite this article: Linneman, D. C., Strickland, C. E., Appriou, D., Rockhold, M. L., Thomle, J. N., Szecsody, J. E., Martin, P. F., Vermeul, V. R., Mackley, R. D., & Freedman, V. L. (2022). Development of a vadose zone advanced monitoring system: Tools to assess groundwater vulnerability. *Vadose Zone Journal*, e20223. https://doi.org/10.1002/vzj2.20223